Nephrol Dial Transplant (2008) 23: 2071–2080
doi: 10.1093/ndt/gfn062
Advance Access publication 14 March 2008

Technical Note

NDT
Nephrology Dialysis Transplantation

A 3D rotary renal and mesenchymal stem cell culture model unveils cell death mechanisms induced by matrix deficiency and low shear stress

Nilly Shimony[1,4], Idit Avrahami[2,4], Raphael Gorodetsky[3], Gregory Elkin[1], Keren Tzukert[1], Lior Zangi[3], Lilia Levdansky[3], Lina Krasny[1] and Yosef S. Haviv[1]

[1]Cell and Gene Therapy Program, Division of Nephrology, Department of Medicine, [2]Department of Medical Engineering AFEKA, Tel Aviv Academic College of Engineering, Tel Aviv and [3]Biotechnology and Radiobiology Laboratory, Department of Oncology, Hadassah-Hebrew University Medical Center, Jerusalem, Israel

Abstract

Background. In epithelial and endothelial cells, detachment from the matrix results in anoikis, a form of apoptosis, whereas stromal and cancer cells are often anchorage independent. The classical anoikis model is based on static 3D epithelial cell culture conditions (STCK).

Methods. We characterized a new model of renal, stromal and mesenchymal stem cell (MSC) matrix deprivation, based on slow rotation cell culture conditions (ROCK). This model induces anoikis using a low shear stress, laminar flow. The mechanism of cell death was determined via FACS (fluorescence-activated cell sorting) analysis for annexin V and propidium iodide uptake and via DNA laddering.

Results. While only renal epithelial cells progressively died in STCK, the ROCK model could induce apoptosis in stromal and transformed cells; cell survival decreased in ROCK versus STCK to 40%, 52%, 62% and 7% in human fibroblast, rat MSC, renal cell carcinoma (RCC) and human melanoma cell lines, respectively. Furthermore, while ROCK induced primarily apoptosis in renal epithelial cells, necrosis was more prevalent in transformed and cancer cells [necrosis/apoptosis ratio of 72.7% in CaKi-1 RCC cells versus 4.3% in MDCK (Madin-Darby canine kidney) cells]. The ROCK-mediated shift to necrosis in RCC cells was further accentuated 3.4-fold by H_2O_2-mediated oxidative stress while in adherent HK-2 renal epithelial cells, oxidative stress enhanced apoptosis. ROCK conditions could also unveil a similar pattern in the LZ100 rat MSC line where in ROCK 44% less apoptosis was observed versus STCK and 45% less apoptosis versus monolayer conditions. Apoptosis in response to oxidative stress was also attenuated in the rat MSC line in ROCK, thereby highlighting rat MSC transformation.

Conclusions. The ROCK matrix-deficiency cell culture model may provide a valuable insight into the mechanism of renal and MSC cell death in response to matrix deprivation.

Keywords: anoikis; mesenchymal stem cells; necrosis; renal cancer; shear stress

Introduction

Upon detachment from the basement membrane, epithelial and endothelial cells undergo anoikis, a term coined to describe a distinct form of apoptosis initiated by loss of matrix-induced signalling. Anoikis was originally described in renal tubular epithelial MDCK cells, keratinocytes and endothelial cells [1,2]. To induce anoikis in anchorage-dependent cells, cell culture plates are typically coated with poly-HEMA [poly(2-hydroxyethyl methacrylate)] [3], an inert polymer impeding cell attachment to the matrix and leading to static 3D cell culture conditions (STCK). However, mesothelial, transformed and stromal cells are relatively resistant to STCK [1–3], thereby requiring alternative techniques to induce anoikis in these cell types. Anchorage independence is a hallmark of carcinoma cells preceding the epithelial-to-mesenchymal transition, i.e. loss of cell–cell adhesion, acquisition of motility and invasion through the basement membrane. These mesenchymal features activate survival signals and may confer cancer cells with resistance to matrix deprivation. Because our preliminary data indicated that the current anoikis model does not induce significant apoptosis in several renal epithelial, cancer and stromal cell lines (Figure 1), we developed a novel, matrix-deficient cell culture model based on slow, 3D rotary cell culture conditions (ROCK model). The 3D cell culture models often include cell culture on microbeads as a means to re-introduce the matrix and avoid cell death [4,5]. A different type of 3D cell culture model without

Correspondence and offprint requests to: Yosef S. Haviv, Kidney Gene and Cell Therapy Program, Division of Nephrology, Department of Medicine, Hadassah-Hebrew University Medical Center, PO Box 12000, Jerusalem 91120, Israel. Tel: +972-2-6776881; Fax: +972-2-6446335, +972-2-6434434; Email: yhaviv@hadassah.org.il
[4]These authors contributed equally to this study.

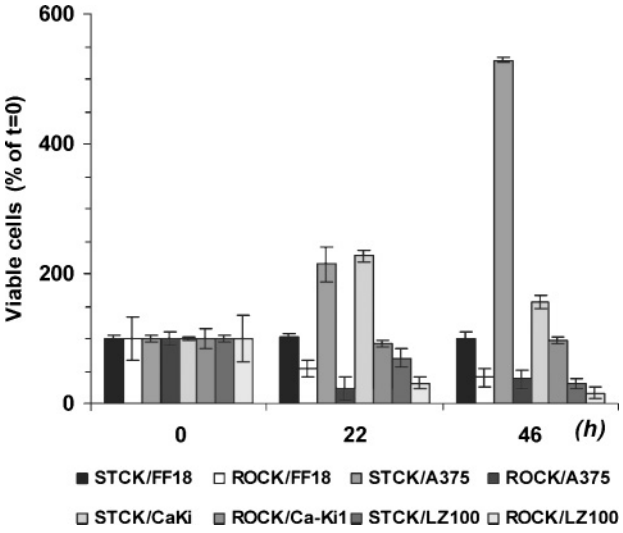

Fig. 1. ROCK versus STCK as a model for matrix detachment and shearing forces. Cells were cultured under slow 3D rotation conditions (ROCK) mimicking circulatory shearing forces or static cell culture conditions in 3D (STCK) using plate coating with the inert polymer poly-HEMA. Cell viability was evaluated with the MTS assay at the indicated times. Viability at time 0 was determined as 100% referral value. Cell titles are as follows: FF18—human foreskin fibroblasts, A375M—high-grade human melanoma cells, CaKi-1—human renal cancer cells and LZ100—rat mesenchymal stem cells.

microbeads is the rotating wall vessel (RWV) cell culture model developed by NASA. The RWV was designed to maintain cell survival and growth by way of an inner oxygenation tube and maintenance of laminar flow resulting from slow horizontal rotation and complete medium tube filling in the absence of air [6]. As a result, suspended cells were reported to survive via aggregation and secretion of their own matrix within the cell aggregate. Cell culture on microbeads in the RWV was suggested to further enhance cell survival [4]. However, as the RWV apparatus is highly complex and costly, its use for 3D cell culture is limited.

Furthermore, even in the RWV model, oxidative and nitrosative stress were observed in colorectal cancer cells [7]. The characteristics of the RWV highlight the principles of fluid dynamics (i.e. shear stress and turbulence) affecting circulating cells. These parameters are determined by the angle of rotation, presence of air, rotation speed and the physical properties of the culture medium. Because in our hands the poly-HEMA model did not induce anoikis in various renal cell lines, we sought to develop a new model to study anoikis in renal cells. To this end, we employed matrix-deprived cell culture under slow rotation cell culture conditions (ROCK). We developed a novel and simple model for anoikis where we changed only two parameters to induce cell death, i.e. the angle of cell culture tubes and the introduction of air into the tube. The rotation speed and medium viscosity and density were left changed relative to microbead culture [4,5]. The ROCK model proved useful to study matrix detachment in a variety of renal and stromal cell lines, inclusive of a rat mesenchymal stem cell (MSC) line.

Materials and methods

ROCK model: a 3D rotary matrix deprivation cell culture model with laminar flow and minimal shear stress

One million cells were suspended in 1.5 ml of the corresponding medium in a 4-ml cryogenic cell tube. The 4-ml tubes were packed in triplicate in a 50-ml polycarbonate tube with no relative motion. All tubes were covered with perforated caps loosely covered by aluminium foil to allow gas exchange while avoiding contamination. Next, the tubes were rotated in a 37°C, water-jacketed, 6% CO_2 incubator on a slowly rotating stand at the rate 15–18 cycles/min at an angle of 20°. Serum depletion [0.5% fetal calf serum (FCS)] was used to eliminate a non-specific survival effect of growth factors in the serum. At the indicated time period, cells were collected and analysed.

Calculation of shear stress and turbulence

Shear stress contrasts with normal stress in applying a parallel or tangential force as opposed to perpendicular force. To calculate maximal shear stress for rotating cells growing on microbeads in fluid full containers, the equation $\tau = 3\mu Vs/2r$ is used, where τ is the shear stress, μ is the cell culture medium viscosity, Vs is the terminal velocity and r is the particle radius. However, as the fluid dynamics for matrix-deprived, suspended cells differ from microbead culture, we first evaluated the type of dynamics in our system. According to Sheritt *et al.* [8], the critical circular speed required for effective centrifugal forces can be calculated in our system [radius (R) = 15 cm] using the formula

$$n = \frac{60s/\text{min}}{2\pi}\sqrt{\frac{g}{R}} = \frac{60s/\text{min}}{2\pi}\sqrt{\frac{g}{0.015\ m}} = 244 \text{ r.p.m.} \quad (1)$$

Because the system velocity is 17–20 cycles/min, the centrifugal force is negligible and the dominant fluid dynamics is 'rolling' or 'circulating'. To evaluate whether the cells were subject to turbulent or laminar flow, we calculated the Reynolds number [Re, reflecting the ratio of inertial forces ($V\rho$) to viscous forces]

Re is defined as

$$Re = \frac{Vd}{\nu}$$

where V is the medium velocity in the rotating container and d equal to $2r$ is the particle diameter. A Reynolds number value <1 indicates creep flow (Stokes flow), $1 < Re < 750$ indicates laminar flow, $800 < Re < 10^4$ indicates transient flow and $Re > 10^4$ is associated with turbulent flow. Because in our system $1 < Re < 750$, the flow is laminar.

To confirm our mathematical calculations, we performed 2D flow simulations in different cross-sections for the velocity of 0.04 rad/s (15 r.p.m.). Using the von Mises criteria $\sigma_{\text{effective}} = (\sigma_1 - \sigma_2)^2$, the effective shear stress on the cells in our system did not exceed 0.1 dyn/cm^2. Thus, the ROCK system allows the study of matrix deprivation under laminar flow and minimal shear stress.

STCK model: static cell culture in 3D for matrix deprivation

Cell culture plates were coated with ethanol-solubilized 2-hydroxyethyl methacrylate (poly-HEMA), an inert polymer impeding cell attachment and inducing a static form of matrix detachment [3]. The poly-HEMA-coated plates were dried overnight, and rinsed as previously reported [1–3]. Control plates were incubated overnight with ethanol only and rinsed before cell culture.

Cell lines

Renal canine tubular epithelial cells (MDCK), human renal tubular epithelial cells (HK-2), transformed human embryonic renal tubular cells stably expressing the adenoviral E1 gene (HEK 293), normal human foreskin fibroblasts (FF) and mouse NIH 3T3 fibroblasts were grown in DMEM, 10% FCS, 1% antibiotics (penicillin–streptomycin) and 1% glutamine. Human cancer kidney cells (CaKi-1) were grown in McCoy's medium with 10% FCS, 1% antibiotics and 1% glutamine. A375 human melanoma cells were grown in RPMI 1640 medium with supplements as above.

MLTR mouse melanoma cells stably expressing the SV40 large T antigen, the human telomerase and the RAS oncogene were kindly provided by Rebecca Perlman and Robert Weinberg (Tufts University, MA, USA). Rat MSC LZ100, a multipotent bone marrow-derived cell line, were grown in MEM α medium supplemented with 10% FCS, 1% antibiotics, 1% glutamine, 1% MEM vitamin solution and 1% MEM non-essential amino acid solution. All culture media, FCS and supplements were purchased from Biological Industries (Beit Haemek, Israel).

Preparation of LZ100 MSC line

Bone marrow from rats was flushed out from the femur and tibia and propagated via needles with serially reduced diameters. To isolate MSC, the whole bone marrow cell population was suspended in 10 ml of DMEM with 20% FCS, 1% antibiotics, 1% glutamine, 1% MEM vitamin solution and 1% MEM non-essential amino acid solution, with 150 μl of packed fibrin microbeads (FMB) in a 50-ml polycarbonate tube as previously described [5,9–11].

Cells isolated following adhesion to FMB were downloaded from the beads to form a monolayer on plastic dishes, expanded and characterized as MSC using both MSC-specific markers and differentiation potential into mesenchymal lineages [10]. To rescue an immortalized line, cells were passaged continuously for up to 100 days (hence the name LZ100) and the spontaneously surviving cells were termed LZ100. This MSC line showed a higher plasticity and differentiation capacity than primary rat MSC.

Assessment of cell growth and viability

The MTS colorimetric assay (Promega, Madison, WI, USA) was used to evaluate the number of living cells by optic density (OD) reading with a plate reader. Initial calibration of OD readings with the number of seeded cells allowed the quantitative measurement of growing cells in the monolayer and in the 3D ROCK model. Viability was also measured with flow cytometry [fluorescence-activated cell sorting (FACS)] analysis (see below) as propidium iodide (PI)-negative, annexin V-negative cells.

Determination of a cell death mechanism

Apoptotic cells were detected by FACS after annexin-V/PI staining as previously described [12,13], probing outer membrane localization of phosphatidyl serine. FITC-conjugated annexin-V FACS gating on positive cells followed counterstaining with PI and gating PI-negative cells (Roche Molecular Biochemicals, Indianapolis, IN, USA). While cells in early apoptotis can still exclude PI from cell entry, PI-positive, annexin V-negative cells are regarded as necrotic cells [12,13]. We thus defined necrotic cells as PI-positive after gating annexin V-negative cells. Viability was determined as PI-negative, annexin V-negative cells, while PI-positive, annexin V-positive cells were regarded as dead cells of indeterminate cause. Results were analysed with Cell Quest software.

DNA fragmentation assay

After culturing under the indicated conditions, cells were harvested, rinsed twice with ice-cold PBS by centrifugation and counted. Cells were passed several times through a 21-gauge needle, and cell debris was sedimented by centrifugation at 12 000 *g* for 15 min at 4°C. DNA was extracted from clear cellular lysates (Qiagen kit + DNase-free RNase), incubated for 2 h at 37°C, and 2 μg of DNA in each lane was then subjected to electrophoresis in 2% agarose gel.

Cell cycle analysis

FACS analysis of cell cycle was performed as previously described [25]. Briefly, after a given period of cell culture in ROCK, LZ100 MSC and MDCK cells were rinsed with ice-cold PBS containing 1% BSA (fraction V; Sigma, St. Louis, MO, USA) by centrifugation at 250 *g* for 5 min at 4°C, and fixed in 70% ethanol with PI. The cellular DNA content was analysed and plotted using a FACStar flow cytometer (Becton, Dickinson and Co., Franklin Lakes, NJ, USA).

Induction and inhibition of oxidative stress

Hydrogen peroxide was used to induce oxidative stress in low (25 mM) and high (75 mM) concentrations, as previously reported [14]. To inhibit mitochondrial cyclophilin D and shuttle of reactive oxygen species (ROS), we employed cyclosporine A (Sigma) at 300 ng/ml. Rapamycin (Sigma) at 50 μM was employed as a control.

Determination of intracellular ROS levels

Oxidative stress in LZ100 cells was measured using FACS analysis. To determine intracellular oxidation, cells were stained with the oxidant-sensitive probe 2′,7′-dichlorofluorescein diacetate (DFC), as previously described [15]. Briefly, after culturing under the various

conditions or at basal levels, cells were incubated with DFC and fluorescence (mean fluorescence channel) was measured using flow cytometry. The shift in fluorescence signal indicated ROS levels indirectly and the cellular oxidative state.

Induction of MSC differentiation

To induce differentiation of rat MSC into different mesenchymal cell phenotypes, 3×10^5 cells/well were plated in six-well plates to reach confluence. The main media used were either 'poor' or 'rich' media. Poor media were based on Dulbecco's modified Eagle's medium with low glucose (1.0 g/ml), 10% FCS, 1% vitamins, 1% non-essential amino acids, 1% glutamine and 1% Pen/Strep (all from Biological Industries). Rich media consisted of Dulbecco's modified Eagle's medium with high glucose (4.5 g/ml), 20% FCS, 1% vitamins, 1% non-essential amino acids, 1% glutamine and 1% Pen/Strep (all from Biological Industries).

The osteogenic differentiation medium consisted of rich media with 50 μg/ml ascorbic acid, 10 mM β-glycerol-phosphate and 10^{-8} M dexamethasone (all from Sigma). Cells were incubated with this medium for 3 weeks with two to three weekly medium exchanges. Nitroso-blue tetrazolium (NBT) staining (DAKO, Glostrup, Denmark) was used to detect osteoblastic differentiation via alkaline phosphatase (AP) activity. NBT (non-coloured) was mixed with β-indolylphosphate (BCIP), and 300 μl of the NBT/BCIP solution was added to the wells and incubated at 37°C in a humidified atmosphere containing 6% CO_2 for 30 min.

At the termination of the reaction, the cells were fixed with 4% paraformaldehyde for 20 min. Alizarin red (Sigma) staining for mineralized osteocyte-secreted matrix red was performed via fixation with cold methanol for 5 min on ice, followed by a 40 mM solution of alizarin-red (pH 4.0) incubation for 15 min at room temperature, rinse with distilled water and air-drying. To induce adipocyte differentiation, poor media were supplemented with 1-methyl-3-isobutylxanthine, 10^{-9} M dexamethasone, 5 mM insulin and 5 mM indomethacin (Stemcell Technologies, Vancouver, Canada). Medium was exchanged twice in a week for 3 weeks. To confirm adipogenesis, 0.25 ml oil red-orange (10 μg/ml, Sigma; staining for 15 min at room temperature and fixation with 4% paraformaldehyde for 20 min) was used to stain intracellular fat droplets red-orange. For chondrocyte differentiation, 10 ng/ml TGF-beta, 6.25 ng/ml insulin and 50 ng/ml ascorbic acid were supplemented to rich media.

Immunofluorescence

Cells were washed gently with 0.05% Tween-20 diluted in PBS (×3) and fixed with fresh 4% paraformaldahyde for 20 min at room temperature. They were then permeabilised with 0.5% Triton X-100 (Sigma) for 7 min. The cells were blocked with 5% bovine serum albumin (BSA) (Biological Industries) in PBS for 60 min at room temperature in slow rotation. They were washed with 0.05% Tween-20 diluted in PBS (×3) and incubated with the primary antibody. The cells were then washed again gently (×3) in PBS with 0.05% Tween-20 and incubated with the relevant secondary antibodies conjugated to Cy2 or Cy3 in 1% BSA buffer, in slow rotation for 45 min in the darkness at room temperature. They were mounted with mounting solution and viewed by fluorescence and light Nomarsky's optics microscopy.

Statistical method

All experiments were performed in triplicates and results were analysed with the *t*-test. $P < 0.05$ was considered statistically significant.

Results

Susceptibility to ROCK and STCK varies in cancer and stromal cell lines

To study the efficiency of the two anoikis models in cells of stromal and renal origin, we cultured cells in ROCK versus STCK. We hypothesized that, unlike the poly-HEMA STCK model, the ROCK model may preclude spheroid formation, known to protect cells from matrix-deprivation death. We thus applied this model to characterize anchorage independence of stromal and renal cells. Because shear stress increases linearly with particle radius, we evaluated the formation of cell aggregates and found that they formed in STCK but not in ROCK (not shown). In STCK, stromal and malignant cells formed spheroids and were relatively resistant to anoikis. In our 3D ROCK anoikis model, we observed that cells were scattered and were more susceptible to cell death than in STCK. Of note, in a different system based on cone and plate apparatus, laminar flow was reported to protect fibroblasts from apoptosis while turbulent flow induced apoptosis [16]. When calculated, the shear stress under ROCK conditions (described in the 'Materials and methods' section) was <0.1 dyn/cm^2, a value lower than the shear stress in the venous system. The Reynolds number, reflecting the smoothness of flow, indicated a laminar flow in our system. Thus, the ROCK model allows the study of matrix deficiency and anoikis via a laminar flow, low shear stress system.

Human cancer cells showed different responses to ROCK. While in STCK, both A375M human melanoma cells and CaKi-1 human renal cancer cells could still proliferate, inhibition of cell survival under ROCK conditions was less dramatic in the CaKi-1 human renal cell carcinoma (RCC) cell line than in the melanoma A375M cell line (Figure 1). We calculated that, relative to STCK, cell survival in ROCK decreased to 40%, 52%, 62% and 7% in human FF, LZ100 rat MSC line, CaKi-1 RCC cells and human A375M melanoma cells, respectively. Thus, the ROCK model may be a more stringent model than STCK to evaluate matrix deprivation in renal epithelial, stromal and cancer cells.

ROCK may unveil the mechanism of renal cell death induced by matrix deprivation

While matrix deprivation in STCK was reported to induce anoikis in a renal epithelial cell line [1,2], cell culture in the horizontally rotating 3D laminar RWV system could

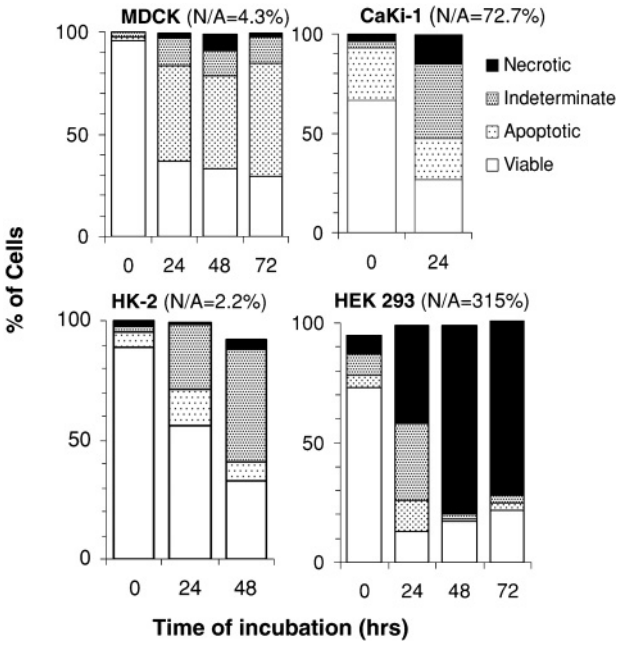

Fig. 2. Apoptotic and necrotic renal cell death induced by ROCK. The renal tubular epithelial cells HK-2 and MDCK, the CaKi-1 RCC cells and the transformed human embryonic kidney cells stably expressing the adenoviral E1 gene (HEK 293) cells were cultured in triplicates in the monolayer ($t = 0$) or in ROCK for either 24 or 48 h followed by PI/annexin V FACS analysis. Necrosis was defined as PI-positive, annexin V-negative, apoptosis was defined as PI-negative, annexin V-positive, viability was defined as PI-negative, annexin V-negative while PI-positive, annexin V-positive cells were defined as indeterminate. The mean of cell number measured in triplicates for each PI–annexin V quadrant is presented as a percentage of total cells, thereby not summing up to 100% in total. The necrosis/apoptosis (*N*/*A*) ratio after 24 h in ROCK is indicated for each cell line.

induce oxidative stress in colorectal cancer cells [7]. Using FACS analysis, we evaluated the cell death mechanism induced by ROCK, where apoptosis was defined as annexin V-positive, PI-negative cells and necrosis as annexin V-negative, PI-positive cells. The cell death mechanism in annexin V-positive, PI-positive cells was regarded as indeterminate. When viability was defined as annexin V-negative, PI-negative cells, the FACS analysis was more sensitive than MTS to detect ROCK-induced cell death (compare CaKi-1 cell death in Figure 1 with Figure 2). The mechanism of cell death in ROCK comprised both apoptosis and necrosis (Figure 2 and Supplementary materials—Figure 1). However, the primary mechanism of cell death appeared to differ between renal epithelial cells and transformed or cancer cells. While apoptosis dominated in renal epithelial MDCK and HK-2 cells, in the transformed renal epithelial HEK 293 and the renal cancer CaKi-1 cells, ROCK-induced necrosis was identified as a major cell death pathway (Figure 2). We therefore calculated a necrosis/apoptosis (*N*/*A*) index after 24 h in ROCK showing 4.3% and 2.2% in renal epithelial MDCK and HK-2, respectively. In contrast, in CaKi-1, E1-transformed HEK 293 and the melanoma MLTR and A375M cells (the latter measured after 48 h), the *N*/*A* ratio was 72.7%, 315%, 100% and 506%, respectively (Figure 2 and Supplementary materials—Figure 1).

To evaluate the development of apoptosis and necrosis in renal cells in a time-dependent manner, we measured the effect of short (2 h) versus prolonged (24 h) cell culture in ROCK on the cell death mechanism in CaKi-1 versus HK-2 cells (Table 1). While in HK-2 cells, the degree of apoptosis was stable after 2 and 24 h in ROCK, in CaKi-1 cells, apoptosis was initially dominant but decreased dramatically by 54% between 2 and 24 h. In contrast, the fraction of necrotic cells increased over time in both cell lines. Thus, CaKi-1 RCC cells are more prone to ROCK-induced necrosis than HK-2 cells.

Of note, in some experiments ROCK increased primarily the fraction of PI-positive, annexin V-positive CaKi-1 cells, rather than purely necrotic CaKi-1 cells (Figure 3 and Table 1). In non-malignant stromal cells, e.g. human FF, the *N*/*A* ratio was 25.4% (Supplementary materials—Figure 1), showing intermediate values between renal epithelial and transformed or cancer cells. Thus, it appears that while in renal epithelial cell lines, apoptosis is the default ROCK-induced cell death pathway, in other cell lines, inclusive of an RCC cell line, necrosis is a dominant cell death mechanism.

The effect of oxidative stress on ROCK-induced cell death

Because the mechanism of ROCK-induced cell death appears to differ between renal epithelial and cancer cells (Figure 2 and Supplementary materials—Figure 1), we next sought to evaluate the effect of oxidative stress in HK-2 and CaKi-1 cells in the monolayer or ROCK using low [25 μM] or high [75 μM] H_2O_2 concentrations (Figures 3 and 4). These concentrations were selected based on previous studies in lymphoma cell lines [14,17]. We also studied the effect of co-incubation with cyclosporine A (CysA), an inhibitor of cyclophilin D, an essential component of the mitochondrial permeability transition pore, mediating oxidative stress. The control for CysA was rapamycin, an inhibitor of the mammalian target of rapamycin (mTOR). While the CaKi-1 RCC line was highly resistant in the monolayer to oxidative stress or therapeutic concentrations of rapamycin, its viability was reduced in ROCK (Figure 3). Furthermore, low and high oxidative stress or rapamycin could not augment ROCK-induced CaKi-1 cell death, indicating that ROCK results in a major breakdown of cellular homeostasis. While CysA had no effect on CaKi-1 cell death in the monolayer or ROCK, it attenuated necrotic cell death induced by the combination of ROCK and oxidative stress (Figure 3). CysA decreased cell death in ROCK with low-dose H_2O_2 by 31.1% and by 24.3% in ROCK with high-dose H_2O_2. Of note, because CysA exerted a similar impact on the degree of both pure necrosis and PI-positive annexin V-positive cells in both the two H_2O_2 concentrations (Figure 3), these dead cells of indeterminate cause may primarily reflect necrosis.

This finding was recapitulated in the combined effect of ROCK and oxidative stress on the indeterminate cell fraction, showing similarity to purely necrotic cells rather than purely apoptotic cells. Of special note, oxidative stress enhanced necrosis (but not apoptosis) in CaKi-1 cells only in ROCK but not in the monolayer (Figure 3). Most of these effects differed dramatically in HK-2 cells (Figure 4), i.e.

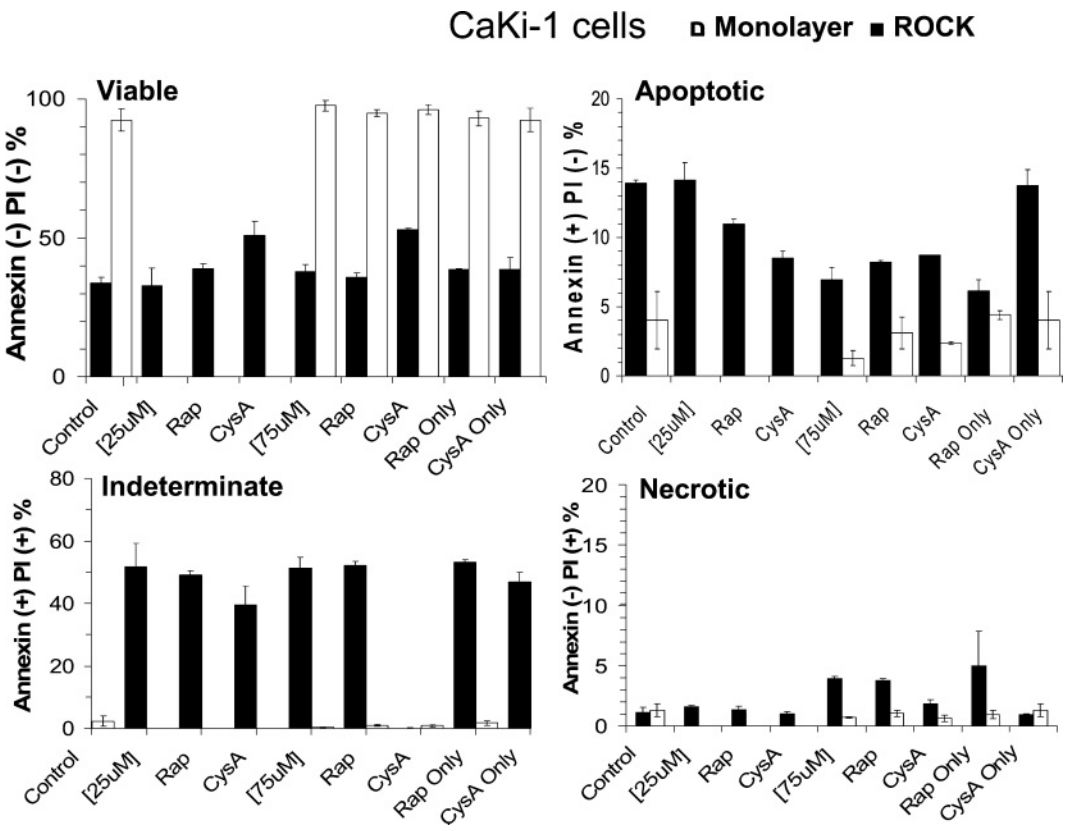

Fig. 3. The effect of oxidative stress on ROCK-induced CaKi-1 RCC cell death. Human CaKi-1 RCC cells were cultured in the monolayer or in ROCK and analysed by FACS as above in Figure 2. To enhance oxidative stress, cells were incubated with low [25 μM] or high [75 μM] H_2O_2 concentrations. For each H_2O_2 concentration, rapamycin (Rap, 50 μM) and cyclosporine A (CysA, 300 ng/ml) were added.

Table 1. Time-dependent ROCK-induced cell death mechanism

Cell death mechanism	HK-2 2-h ROCK	HK-2 24-h ROCK	CaKi-1 2-h ROCK	CaKi-1 24-h ROCK
Apoptosis	11 ± 2.08%	13 ± 0.33%	37 ± 2.48%*	17 ± 3.29%*
Necrosis	2 ± 1.97%	12 ± 3.45%	7 ± 2.17%	15 ± 6.84%
Indeterminate	11 ± 0.56%	44 ± 1.01%	18 ± 1.57%	36 ± 1.92%

*$P < 0.05$ for 2- to 24-h decrease in CaKi-1 apoptosis versus HK-2.

the renal epithelial HK-2 cells were sensitive in the monolayer to oxidative stress and therapeutic concentrations of rapamycin, and CysA did not attenuate HK-2 cell death and necrosis in ROCK with H_2O_2. Also, HK-2 cells in ROCK were shifted to necrotic cell death by oxidative stress, while RCC cells were practically resistant to H_2O_2 oxidative stress and required ROCK to die.

To confirm that renal epithelial HK-2 cells but not the RCC CaKi-1 cells are prone to apoptosis induced by ROCK and enhanced by oxidative stress, we also evaluated DNA laddering, another marker of apoptosis. In HK-2 cells, ROCK resulted in DNA laddering augmented by oxidative stress (Figure 5). In contrast, CaKi-1 renal cancer cells did not show DNA laddering in ROCK even when combined with high oxidative stress. Thus, using both FACS and DNA electrophoresis we show that ROCK induces distinct cell death mechanisms in renal epithelial versus an RCC cell line.

ROCK can identify cell cycle abnormalities in MSC

Prior to homing to the kidney, systemic delivery of MSC mandates matrix independence in the circulation. We thus employed the ROCK model to study the cell survival, anoikis and death mechanism of matrix-deprived MSC. Upon matrix detachment in STCK and ROCK, the rat MSC line LZ100 cells died profusely, where survival after 46 h was 31% and 16.3% in STCK and ROCK, respectively (Figure 1). To induce apoptosis, we cultured LZ100 cells in 0.5% serum under the monolayer, STCK and ROCK conditions.

Viability was very low after 48 h under all three conditions, but ROCK suppressed apoptosis in LZ100 when compared to the monolayer and STCK (Figure 6a), correlating with an accumulation of ROS induced by ROCK (Figure 6B). LZ100 cells showed in ROCK 44% less apoptosis than in STCK and 45% less apoptosis than under monolayer conditions (Figure 6A). These features were

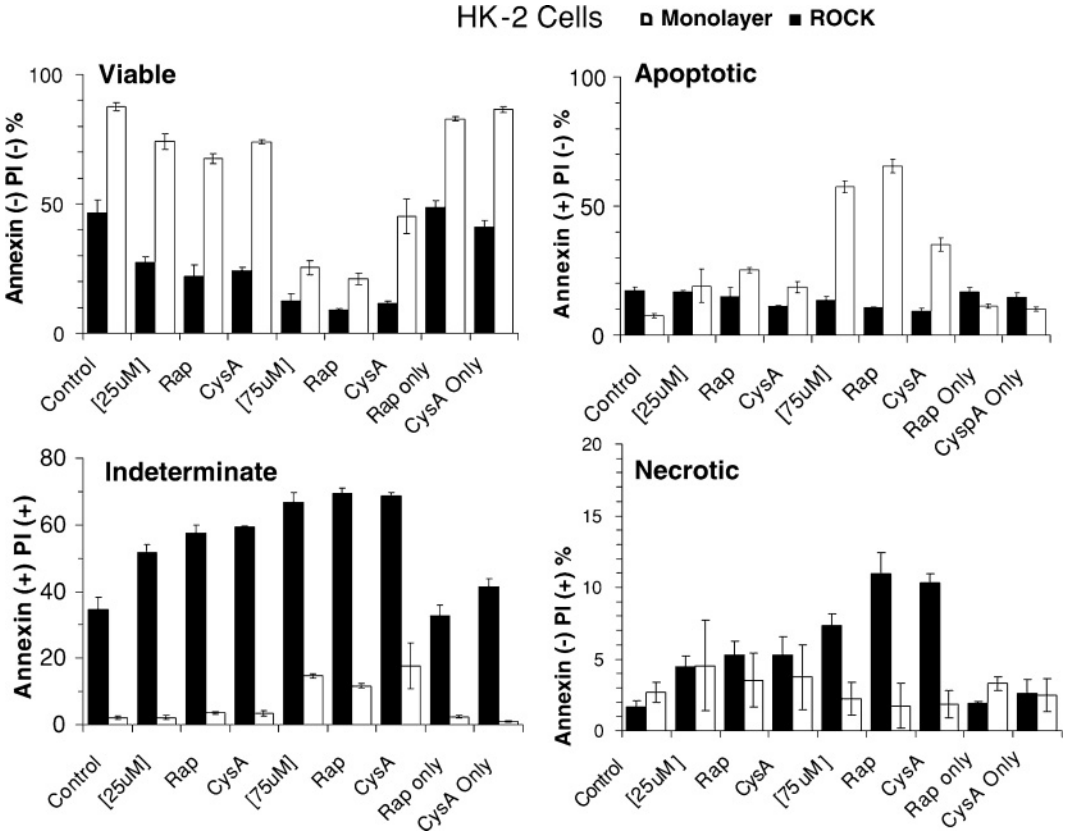

Fig. 4. The effect of oxidative stress on ROCK-induced HK-2 renal epithelial cell death. Human HK-2 renal epithelial cells were cultured and analysed exactly as above in Figure 4. To enhance oxidative stress, cells were incubated with low [25 μM] or high [75 μM] H_2O_2 concentrations. For each H_2O_2 concentration, rapamycin (Rap, 50 μM) and cyclosporine A (CysA, 300 ng/ml) were added.

reminiscent of transformed cells where we had observed attenuated ROCK-induced apoptosis (Figure 2 and Supplementary materials—Figure 1), and of the lack of H_2O_2-induced apoptosis in renal cancer cells, unlike renal epithelial cells (Figure 5). We thus next evaluated whether LZ100 may show features of transformed cells. To this end, we studied the effect of ROCK on the cell cycle of LZ100 (Figure 7). While ROCK shifted 15% of MDCK cells to the subG1 phase, it drove only 7.3% of LZ100 to subG1 phase, indicating again a low apoptotic response in MSC to ROCK. Cell cycle analysis of adherent LZ100 in the monolayer revealed an aberrantly high G2/M phase indicating a high mitotic rate (Figure 7). These findings correlated with cellular transformation characterized by an abnormal karyotype showing a high degree of aneuploidy (Supplementary materials—Figure 2) and unlimited growth potential over 70 passages in culture (not shown). The LZ100 rat MSC cells nevertheless retained their capacity to function as pluripotent cells and differentiate into adipocytes, osteocytes and neurons (Supplementary materials—Figure 3). Thus, the ROCK model could highlight an abnormally low degree of apoptotic response to matrix deficiency in LZ100 MSC cells, correlating with cell transformation.

Discussion

Previous experimental *in vitro* models have addressed primarily anchorage dependence of epithelial cells via coating cell culture plates with poly-HEMA and induction of cell spheroids in the STCK model [1,2]. However, because stromal and carcinoma cells undergoing epithelial-to-mesenchymal transition show anchorage independence [1,2], and even cell proliferation in STCK [3], a relevant model is required to induce matrix deprivation and cell death in these cells. To this end, we developed the ROCK model to study the effect of matrix deprivation on renal and stromal cells. This model allows the efficient induction of anoikis in a low shear, laminar rotational flow 3D cell culture model. We show here that fibroblasts and an RCC cell line, but not renal epithelial cells, are relatively resistant to STCK, requiring ROCK to efficiently induce matrix-deprived cell death. One possible cause for this observation may include the natural cell–cell adhesion property of epithelial cells that is maintained in STCK but not in ROCK. In contrast, stromal and malignant cells usually do not form cell–cell adhesion and are not based on a basement membrane, a mechanism possibly accounting for better survival in STCK.

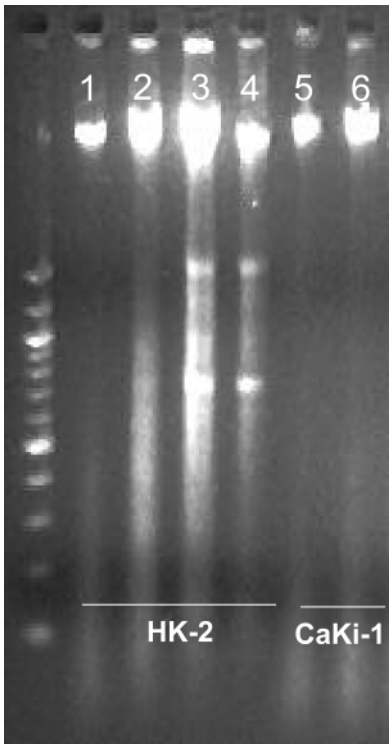

Fig. 5. The effect of oxidative stress on ROCK-induced renal cell death. DNA gel electrophoresis showing apoptosis in HK-2 but not in CaKi-1 cells. Cells were cultured in the monolayer or in ROCK for 2 h with 0.5% serum, with or without H_2O_2. After 2 h, cells were collected, DNA extracted and 2 μg was loaded in each lane. Lanes are: (1) HK-2 monolayer, (2) HK-2 in ROCK, (3) HK-2 in ROCK + 25 μM H_2O_2, (4) HK-2 in ROCK + 75 μM H_2O_2, (5) CaKi-1 in ROCK and (6) CaKi-1 in ROCK + 75 μM H_2O_2.

The ROCK model could provide valuable information regarding apoptosis or necrosis as the primary cell death mechanism in a variety of cell types, generally correlating with the cell transformation status. Activation of non-receptor tyrosine kinases in transformed cells was previously shown to confer anoikis resistance via different pathways, e.g. v-SRC [1], phosphorylated FAK [18], phosphorylated SRC, the PI3-kinase/AKT pathway [19] or ERK [20]. Our data show that in addition to anoikis, necrosis is a major cell death mechanism induced by anoikis in transformed cells. This conclusion is based on the observation that renal epithelial cells showed primarily ROCK-induced apoptosis, while malignant and transformed cells manifested substantial necrosis under ROCK conditions.

Two possible mechanisms may account for a higher rate of necrosis in transformed cells. First, upregulation of intrinsic anti-apoptotic cellular pathways in transformed cells [21] may shift these cells to necrosis rather than apoptosis upon derangement of cell homeostasis by matrix deprivation. Furthermore, following the report that oxidative stress enhances necrosis in lymphoma cells [17], we observed that oxidative stress induces apoptosis in the epithelial HK-2 cell line, in contrast to necrosis in CaKi-1 cells. The combination of matrix deprivation in ROCK and oxidative stress further accentuated the difference in cell death in the epithelial versus malignant renal cell lines. Thus, while oxidative stress drove HK-2 cells to apoptotic cell death in the monolayer, it had practically no effect on adherent CaKi-1 cells. In contrast, while under ROCK conditions CaKi-1 cells died profusely of both apoptosis and necrosis, oxidative stress, combined with ROCK enhanced necrosis but decreased apoptosis. Recent data suggest that FLIP, an endogenous inhibitor of Fas death receptor signalling, and TRAIL, the ligand of DR5, may confer resistance to anoikis in prostate cancer and colorectal cancer cells, respectively [22,23]. It will be of interest to examine whether FLIP also plays a role in the resistance of circulating renal cancer cells to matrix deprivation. Second, oxidative stress, resulting from matrix deprivation [7], may cause depletion of ATP. Because apoptosis is an energy-requiring process, ATP depletion may shift cells to necrosis [17]. Transformed cells, having a higher metabolic rate, may be thus more prone to necrosis. In this regard, because oxidative and nitrosative stress may circumvent apoptosis resistance in cancer cells while sparing normal cells [24,25], induction of alternative pathways of renal cancer cell death may circumvent apoptosis resistance.

Our original observation of necrosis as a primary death pathway in matrix-deprived cancer cells is supported by the results of Jessup *et al*. [7]. While these authors referred only to suspension-induced apoptosis, their flow cytometry results clearly show necrosis in colorectal cells suspended in the RWV model, as evident by 44% PI-positive, annexin V-negative cells versus only 2% PI-negative, annexin V-positive cells. Furthermore, these authors specifically noted that ROCK-induced colorectal cancer cell death was not associated with DNA degradation, a typical finding in apoptosis [7]. This finding is in accord with our finding of enhancement of DNA degradation by oxidative stress in renal epithelial HK-2 cells in ROCK, but not in RCC CaKi-1 cells in ROCK (Figure 5). Thus, necrotic cell death may be an important general cancer cell death mechanism under matrix-deficiency conditions, where enhancement of cancer cell oxidative stress may be a potential therapeutic target. This hypothesis is further supported by the previous report that lymphoma cells exposed to severe oxidative stress are shifted from apoptosis to necrosis [17].

MSC have been suggested as renoprotective agents in the context of acute renal failure [26]. Because we observed in the rat MSC LZ100 a lower degree of ROCK-induced apoptosis than in STCK or the monolayer, it was of interest to assess their cell cycle response to ROCK. LZ100 displayed a baseline deranged cell cycle and an abnormal, low apoptotic response to ROCK. These abnormalities correlated with the karyotype aneuploidy of LZ100. Thus, despite their capacity to differentiate into various mesenchymal lineages, showing even higher plasticity and differentiation capacity than other primary rat MSC lines, LZ100 transformation raises concern regarding the use of high-passage MSC for clinical purposes, as has been recently suggested for mouse MSC that became spontaneously malignant [27].

CysA showed a dual effect on renal cells. In the HK-2 renal tubular epithelial cells, CysA enhanced apoptosis (Figure 4) while in RCC cells, it attenuated the additive effect of oxidative stress on ROCK-induced necrotic cell death (Figure 3). These findings may be compatible with an inhibitory role of CysA on cyclophilin D, an essential

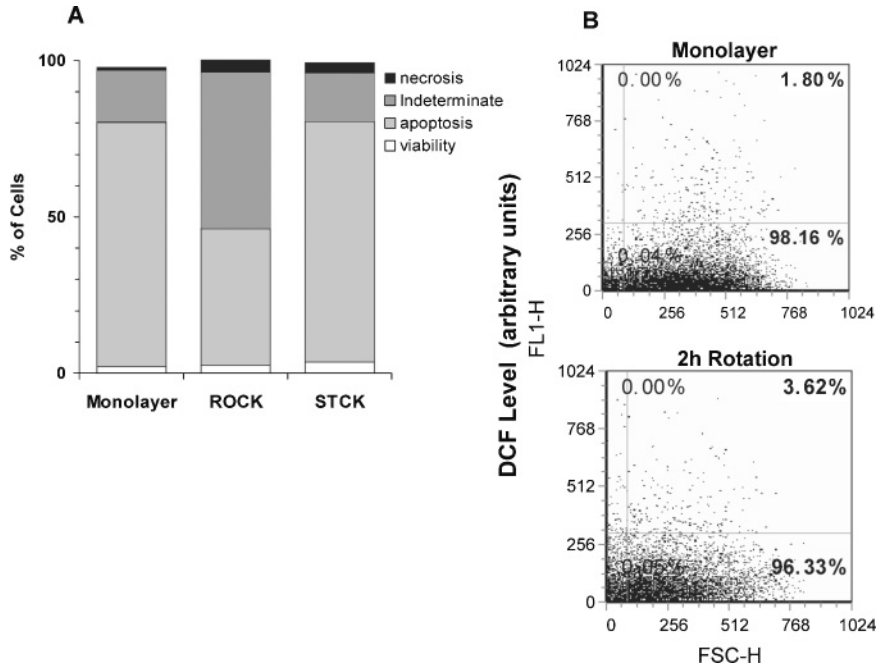

Fig. 6. Mechanism of cell death of rat MSC LZ100 cells in ROCK. (**A**) To induce apoptosis, LZ100 were cultured for 48 h in 0.5% serum (LZ100 normally require 20% serum to proliferate) on the monolayer, STCK or in ROCK. Apoptosis/necrosis/viability were determined using PI/annexin V FACS as above in Figures 2 and 3. (**B**) ROCK-induced increase in reactive oxygen species (ROS) was measured in LZ100 indirectly via a shift in DCF fluorescence using FACS analysis as described in the 'Materials and methods' section.

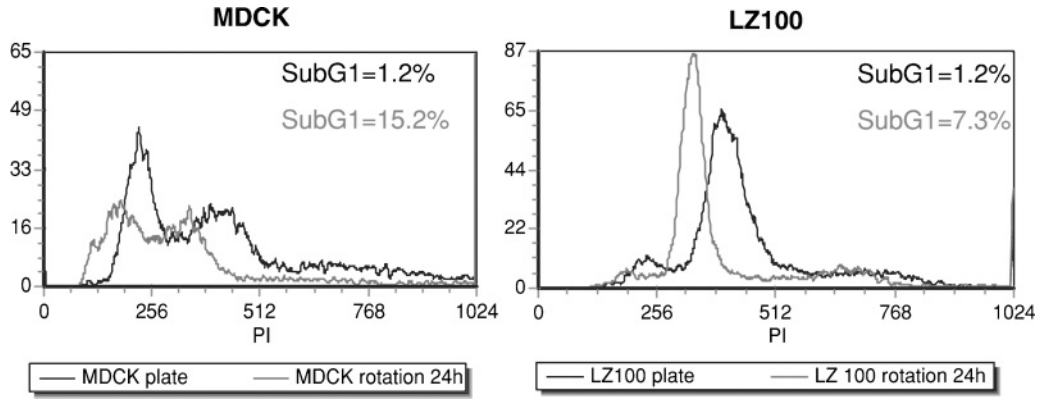

Fig. 7. Aberrant LZ100 cell cycle response to ROCK. Cell cycle in the LZ100 MSC line and control MDCK cells, in the monolayer or in ROCK for 24 h, was analysed and plotted via measurement of PI-labelled cellular DNA content using a flow cytometer. The control range of cells in the subG1 phase was determined for cells in the monolayer. While in the monolayer MDCK cells maintained a normal low G2/M to G1/G0 ratio, LZ100 demonstrated an aberrantly high number of cells in G2/M phase. ROCK-induced apoptosis cells in subG1 phase were lower in number in LZ100 versus MDCK cells.

component of the mitochondrial permeability transition pore. CysA has been shown before to protect cells from oxidative stress-induced necrotic cell death [28]. This effect may explain the differential effect of CysA in HK-2 and CaKi-1 cells. In the renal epithelial cells, high-dose H_2O_2 caused apoptotic cell death only in the monolayer, precisely where CysA exerted its inhibitory effect and attenuated oxidative stress-induced apoptotic cell death (Figure 4). In contrast, in CaKi-1 cells H_2O_2 enhanced necrotic cell death only in ROCK, precisely where CysA exerted its inhibitory effect and attenuated oxidative stress-induced necrotic cell death (Figure 3). Of special note, oxidative stress enhanced necrosis and not apoptosis in CaKi-1 cells in ROCK but not in the monolayer (Figure 3), suggesting again that circulating RCC cells may be more susceptible to necrosis than to apoptosis.

In conclusion, we describe the effects of matrix deprivation under low shear stress in a 3D cell culture on renal and stromal cells. We show that various cell types may die in ROCK from either necrosis or apoptosis and that oxidative stress may shift ROCK-induced cell death to necrosis in transformed cells. These findings may be of relevance for future studies on the cell death mechanisms induced by matrix deprivation.

Supplementary material

Supplementary material is available online at http://ndt.oxfordjournals.org

Acknowledgements. This study was supported by the German-Israeli Foundation (grant no. 817/2004), Israeli Science Foundation (grant no. 573/2003) and the Hadassah Medical Organization Women's Health Fund.

Conflict of interest statement. None declared.

References

1. Frisch SM, Francis H. Disruption of epithelial cell-matrix interactions induces apoptosis. *J Cell Biol* 1994; 124: 619–626
2. Meredith JE, Fazeli B, Schwartz MA. The extracellular-matrix as a cell-survival factor. *Mol Biol Cell* 1993; 4: 953–961
3. Folkman J, Moscona A. Role of cell-shape in growth-control. *Nature* 1978; 273: 345–349
4. Hammond TG, Hammond JM. Optimized suspension culture: the rotating-wall vessel. *Am J Physiol Renal Physiol* 2001; 281 F12–F25.
5. Gorodetsky R, Vexler A, Levdansky L *et al*. Fibrin microbeads (FMB) as biodegradable carriers for culturing cells and for accelerating wound healing. In: A. Hollander and P. Hatton (eds). *Biopolymer Methods in Tissue Engineering*. Humana Press, Totowa, NJ, USA, 2004, 11–23
6. Jessup JM, Goodwin TJ, Spaulding G. Prospects for use of microgravity-based bioreactors to study three-dimensional host-tumor interactions in human neoplasia. *J Cell Biochem* 1993; 51: 290–300
7. Laguinge LM, Lin SL, Samara RN *et al*. Nitrosative stress in rotated three-dimensional colorectal carcinoma cell cultures induces microtubule depolymerization and apoptosis. *Cancer Res* 2004; 64: 2643–2648
8. Sherritt RG, Chaouki J, Mehrotra AK *et al*. Axial dispersion in the three-dimensional mixing of particles in a rotating drum reactor. *Chem Eng Sci* 2003; 58: 410–415
9. Kassis I, Zangi L, Rivkin R *et al*. Isolation of mesenchymal stem cells from G-CSF-mobilized human peripheral blood using fibrin microbeads. *Bone Marrow Transplant* 2006; 37: 967–976
10. Gurevich O, Vexler A, Marx G, *et al*. Fibrin microbeads for isolating and growing bone marrow-derived progenitor cells capable of forming bone tissue. *Tissue Eng* 2002; 8: 661–672
11. Zangi L, Rivkin R, Kassis I *et al*. High-yield isolation, expansion, and differentiation of rat bone marrow-derived mesenchymal stem cells with fibrin microbeads. *Tissue Eng* 2006; 12: 2343–2354
12. Baatout S, Herradji H. Cytometric methods to analyze radiation effects. *J Biol Regul* 2004; 18: 101–105
13. Candido KA, Shimizu K, McLaughlin JC *et al*. Local administration of dendritic cells inhibits established breast tumor growth: implications for apoptosis-inducing agents. *Cancer Res* 2001; 61: 228–236
14. Englert RP, Shacter E. Distinct modes of cell death induced by different reactive oxygen species—amino acyl chloramines mediate hypochlorous acid-induced apoptosis. *J Biol Chem* 2006; 277: 20518–20536
15. Amer J, Fibach E. Chronic oxidative stress reduces the respiratory burst response of neutrophils from beta-thalassaemia patients. *Br J Haematol* 2005; 129: 435–441
16. Graf R, Apenberg M, Freyberg M *et al*. A common mechanism for the mechanosensitive regulation of apoptosis in different cell types and for different mechanical stimuli. *Apoptosis* 2003; 8: 531–538
17. Lee Y, Shacter E. Oxidative stress inhibits apoptosis in human lymphoma cells. *J Biol Chem* 1999; 274: 19792–19798
18. Frisch SM, Ruoslahti E. Integrins and anoikis. *Curr Opin Cell Biol* 1997; 9: 701–706
19. Diaz-Montero CM, Wygant JN, McIntyre BW. PI3-K/Akt-mediated anoikis resistance of human osteosarcoma cells requires Src activation. *Eur J Cancer* 2006; 42: 1491–1500
20. Zeng QH, Chen SQ, You ZB *et al*. Hepatocyte growth factor inhibits anoikis in head and neck squamous cell carcinoma cells by activation of ERK and Akt signaling independent of NF kappa B. *J Biol Chem* 2002; 277: 25203–25208
21. Hanahan D, Weinberg RA. The hallmarks of cancer. *Cell* 2000; 100: 57–70
22. Mawji IA, Simpson CD, Hurren R *et al*. Critical role for Fas-associated death domain-like interleukin-1 converting enzyme-like inhibitory protein in anoikis resistance and distant tumor formation. *J Natl Cancer Inst* 2007; 99: 811–822
23. Samara RN, Laguinge LM, Jessup JM. Carcinoembryonic antigen inhibits anoikis in colorectal carcinoma cells by interfering with TRAIL-R2 (DR5) signaling. *Cancer Res* 2007; 67: 4774–4782
24. Lebedeva IV, Washington I, Sarkar D *et al*. Strategy for reversing resistance to a single anticancer agent in human prostate and pancreatic carcinomas. *Proc Natl Aacd Sci* 2007; 104: 3484–3489
25. Naito M, Hashimoto C, Masui S *et al*. Caspase-independent necrotic cell death induced by a radiosensitizer, 8-nitrocaffeine. *Cancer Sci* 2004; 95: 361–366
26. Morigi M, Imberti B, Zoja C *et al*. Mesenchymal stem cells are renotropic, helping to repair the kidney and improve function in acute renal failure. *J Am Soc Nephrol* 2004; 15: 1794–1804
27. Zhou YF, Bosch-Marce M, Okuyama H *et al*. Spontaneous transformation of cultured mouse bone marrow-derived stromal cells. *Cancer Res* 2006; 66: 10849–10854
28. Li L, Han W, Gu Y *et al*. Honoikol induces a necrotic cell death through the mitochondrial permeability transition pore. *Cancer Res* 2007; 67: 4894–4903

Received for publication: 18.7.07
Accepted in revised form: 25.1.08